



Bensulide exposure causes cell division cycle arrest and apoptosis in porcine trophectoderm and uterine luminal epithelial cells

Miji Kim ^{a,1}, Junho Park ^{a,1}, Hojun Lee ^a, Whasun Lim ^{b,*}, Gwonhwa Song ^{a,**}

^a Institute of Animal Molecular Biotechnology and Department of Biotechnology, College of Life Sciences and Biotechnology, Korea University, Seoul 02841, Republic of Korea

^b Department of Biological Sciences, Sungkyunkwan University, Suwon 16419, Republic of Korea



ARTICLE INFO

Keywords:

Cytotoxicity
Programmed cell death
Mitochondrial dysfunction
Calcium homeostasis
Implantation

ABSTRACT

As the use of herbicides in agriculture has increased worldwide, the importance of identifying unexpected toxic effects on non-target organisms is emerging. Bensulide is used on various agricultural crops as an organophosphate herbicide; however, it can pose a high risk to non-target organisms because of its long half-life and accumulative potential. Despite its high risk, the hazardous effects of bensulide on implantation and mechanisms in cells have not been reported. Therefore, in this study, intracellular mechanisms and potential risk of implantation failure were identified in porcine trophectoderm (pTr) and uterine luminal epithelial (pLE) cells derived from pigs with human-like molecular mechanisms in implantation. The LC₅₀ values of bensulide were 5.21 mg/L in pTr cells and 6.49 mg/L in pLE cells. Both cell lines were exposed to bensulide at concentrations <5 mg/L in subsequent experiments. Treatment with 5 mg/L bensulide activated ERK1/2 and JNK. Disrupted mitochondrial membrane potentials of both cell types were identified. In addition, mitochondrial Ca²⁺ concentration increased to 261.24% and 228.04% in pTr and pLE cells, respectively, and cytoplasmic Ca²⁺ concentrations decreased by approximately 50% in both cell types. The abnormal regulation of various intracellular environments by bensulide causes cell division cycle arrest and apoptosis. Finally, 5 mg/L bensulide inhibited transcription of implantation-related genes. Collectively, our results suggest that bensulide may interrupt implantation during early pregnancy by disrupting maternal-fetal interaction.

1. Introduction

Pesticides are used worldwide because they maximize agricultural production and generate economic benefits through pest control. However, owing to the unexpected hazardous effects of pesticides, various countries are regulating pesticide use by evaluating safety (Donley, 2019). Bensulide, an organophosphate herbicide, is used in vegetable, legume, and garlic agriculture as a lipid synthesis and cell division inhibitor (Antonious, 2010). In the US, 0.5–0.7 million pounds of bensulide is used per year, according to the Pesticide National Synthesis Project of the US Geological Survey (Bensulide, 2006). In Boston, Philadelphia, and Rochester, the mean runoff concentrations of bensulide ranged 0.082–0.175 mg/L (Haith and Rossi, 2003). In addition, bensulide was detected in more than one-third of the surface water samples in California, with a highest detected value of 52.3 µg/L

(Nakhjavani et al., 2021). A half-life of approximately 210 days and high organic carbon absorption coefficient (K_{oc}) of 3900 mL/g suggest that bensulide retention in the soil is high, and may lead to exposure to non-target organisms, causing various toxic effects (Haith and Rossi, 2003; Safety et al., 2019). Furthermore, bensulide has been detected in urine samples of humans with high risks of exposure to pesticides (Lopez-Garcia et al., 2019). This indicates the ingestion and retention of bensulide in humans that can cause adverse effects in the body.

Previous studies have been conducted to identify the hazardous effects of bensulide on non-target organisms owing to its long half-life, the potential for adsorption by organisms, and the possibility of outflow. Bensulide (1000 mg/L) reduces the hatching rate of Japanese quails (Shellenberger et al., 1965). The mortality of channel catfish (*Ictalurus punctatus*) is reported to be 10% after exposure to 10 mg/L bensulide for 48 h (McCorkle et al., 1977). In addition, bensulide inhibits the growth

* Corresponding author at: W.Lim, Department of Biological Sciences, College of Science, Sungkyunkwan University, Suwon 16419, Republic of Korea.

** Correspondence to: G. Song, Department of Biotechnology, College of Life Sciences and Biotechnology, Korea University, Seoul, 02841, Republic of Korea.

E-mail addresses: wlim@skku.edu (W. Lim), ghsong@korea.ac.kr (G. Song).

¹ These authors contributed equally to the study.

of mouse leukemia and lymphoma cells, and cell growth is arrested at 40 mg/L bensulide exposure *in vitro* (Zilkah et al., 1981). Furthermore, bensulide causes miscarriages in rabbits by disrupting vascular development during placental formation (Kleinsteuer et al., 2011). Additionally, it is reported that organophosphate herbicides can cause reproductive toxicity throughout pregnancy (from early pregnancy to childbirth) (Hu et al., 2020; Eskenazi et al., 2004). As herbicides are classified according to their respective chemical structures and modes of action, it is suggested that bensulide, an organophosphate herbicide, may also negatively affect various pregnancy stages (Mallick et al., 2023). However, there is no detailed description of the cellular mechanisms underlying the adverse effects of bensulide on female reproduction, especially during early pregnancy.

To determine the effects of bensulide on intracellular mechanisms in implantation-related cells, we required the following *in vitro* models: 1) *in vitro* cells closely related to implantation, 2) cell lines that did not impair implantation-related cell characteristics, and 3) derived from animal models that can reflect the implantation mechanisms in humans. The pTr and pLE cell lines are derived from trophoblasts of porcine conceptuses and porcine uterus, respectively. In addition, both cell lines fully reflect functions related to implantation performed *in vivo* (Ka et al., 2001; Wang et al., 2000). Porcine models have molecular mechanisms similar to those involved in early pregnancy in humans. Therefore, a porcine model was used to study the mechanisms of implantation in human female reproduction, despite differences in implantation and placental structure (Baryla et al., 2019). In addition, both cell types have been utilized in various *in vitro* studies to identify intracellular toxicity mechanisms induced by pesticides and to evaluate their effects on implantation processes (Park et al., 2022; Kim et al., 2022; Park et al., 2021). Hence, this study used porcine trophectoderm (pTr) and uterine luminal epithelial (pLE) cell lines to determine the detailed intracellular mechanisms of adverse effects of bensulide on implantation in early pregnancy *in vitro*.

In the present study, we hypothesized that bensulide induces toxic effects in implantation-related cells. Therefore, programmed cell death, proliferation rate, and cell division cycle progression were analyzed following bensulide exposure. In addition, Ca²⁺ homeostasis, mitochondrial function, and related gene and protein expression and activation were evaluated to elucidate the intracellular mechanisms involved in bensulide toxicity. Finally, cell functions were evaluated through implantation-related gene expression analysis and cell migration and aggregation ability measurements. This study identified the mechanisms underlying the effects of bensulide on each cell line. This study provides a blueprint for the potential adverse effects of implantation.

2. Materials and methods

2.1. Cell culture

pTr and pLE cell lines were established by Dr. Fuller W. Bazer et al. (Texas A&M University), who generously provided the cell lines for use in the present study. DME/F12 1:1 growth medium (catalog no. SH30023.01, HyClone, Utah, USA) supplemented with 10% fetal bovine serum (FBS; Catalog number SH30919.03, HyClone) was used to culture the cells. Both cell lines were cultured to 70% confluence in a 5% CO₂ incubator at 37 °C in air humidified with sterile distilled water. Moscona's EDTA and 0.05% trypsin-EDTA were used to harvest cells for further experiments.

2.2. Chemicals and reagents

We obtained bensulide (O, O-diisopropyl S-2-phenylsulfonylaminoethyl phosphorodithioate; purity: ≥95%) from Sigma-Aldrich (Cat No. 31469, St. Louis, MO, USA) and dissolved it in dimethyl sulfoxide (DMSO) before use. A bensulide stock solution was

Table 1
Reagents and antibodies used in this study.

Name	Catalog No.	Source
Bensulide	31,469	Sigma-Aldrich
Bovine serum albumin (BSA)	A4919	Sigma-Aldrich
Fetal bovine serum (FBS)	SH30919.03	HyClone
p-ERK1/2 (Thr ²⁰² /Tyr ²⁰⁴)	9101	Cell Signaling Technology
p44/42 MAPK (ERK1/2)	4695	Cell Signaling Technology
p-SAPK/JNK (Thr ¹⁸³ /Tyr ¹⁸⁵)	4668S	Cell Signaling Technology
SAPK/JNK	9252	Cell Signaling Technology
Anti-GAPDH	OAEA00006	Aviva Systems Biology
PCNA (PC10)	sc-56	Santa Cruz
Cyclin D1 (H-295)	sc-753	Santa Cruz
β-actin	sc-47778	Santa Cruz
Goat anti-rabbit IgG-HRP	sc-2004	Santa Cruz
Goat anti-mouse IgG-HRP	sc-2005	Santa Cruz

Table 2
Primer sequences for analysis of mRNA transcription.

Gene (size)	Primer sequence (5' → 3')
BAX (113 bp)	Forward: 5'-TTGCTTCAGGGTTTCATCC-3' Reverse: 5'-GACACTCGCTCACTCTTG-3'
BAK (128 bp)	Forward: 5'-CTGGACTCAGGGATCTGG-3' Reverse: 5'-TGGGAGCAAGTAGAACAGG-3'
ESR1 (75 bp)	Forward: 5'-GATGATCAGTCCTGTGG-3' Reverse: 5'-CTCACTGAGGGCTGTGGTAG-3'
ESR2 (105 bp)	Forward: 5'-GCTCATCTTGCTCCAGACC-3' Reverse: 5'-CGAACCTTGAAGTCGTGC-3'
PTGIR (148 bp)	Forward: 5'-TGGCATCATGACTGTG-3' Reverse: 5'-GAAAAGGATGAAGACCCAAGG-3'
CASP1 (148 bp)	Forward: 5'-CTGGTGCTCATGTCATGG-3' Reverse: 5'-TGATCACCTGGTTGTCC-3'
RXFP1 (98 bp)	Forward: 5'-TATTTGCTCTGGGAGTGG-3' Reverse: 5'-TTGCAGTGAAGCAACTGAGG-3'

prepared at a concentration of 10 g/L and 20 g/L. All experimental and control groups were exposed to the same volume of the vehicle (0.05% DMSO). Information regarding antibodies and other reagents is presented in Table 1.

2.3. Analysis of cell viability

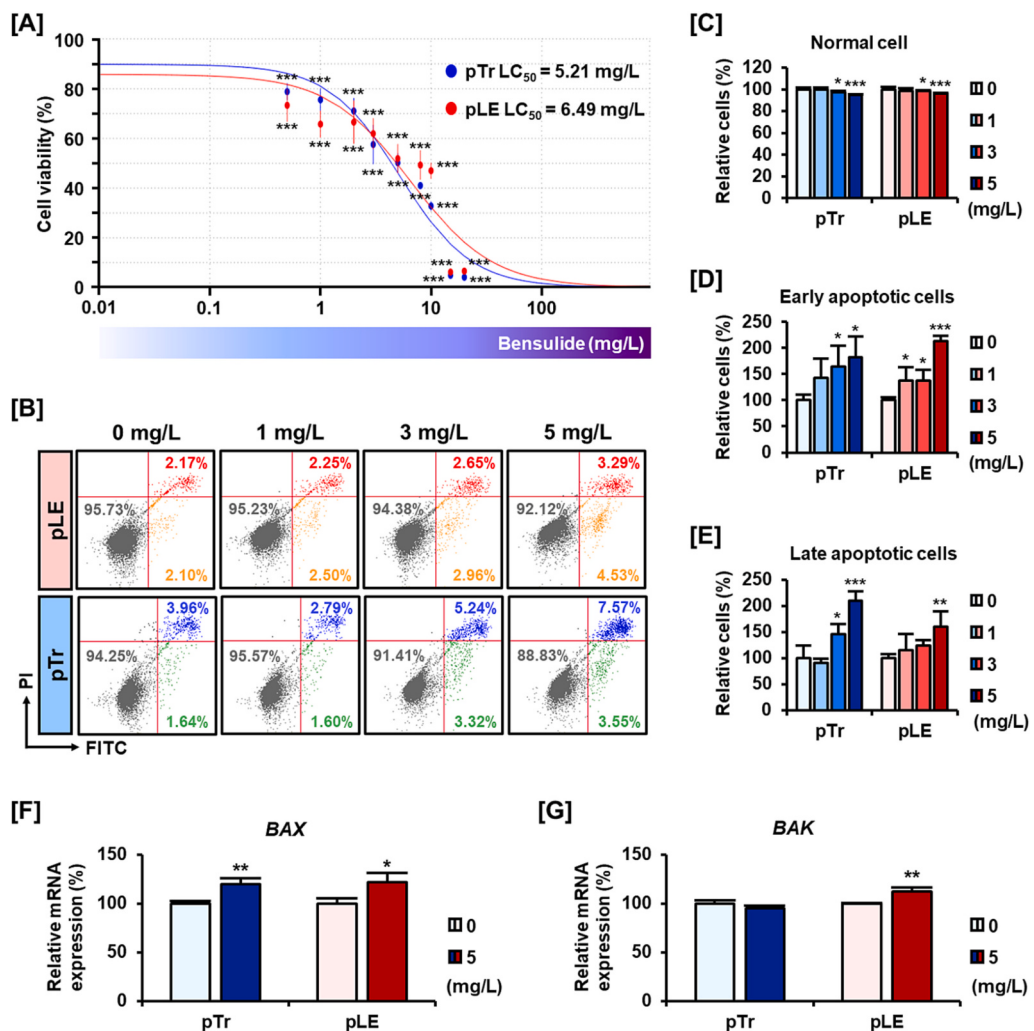
The viability of both cell types was analyzed using Cell Proliferation Kit I (Catalog No. 11465007001, Roche, Basel, Switzerland). Cells exposed to bensulide for 48 h were incubated with an MTT labeling reagent for 2 h. Following incubation, a solubilization solution was added, and the optical absorbance of formazan crystals was detected. The LC₅₀ was determined using the Quest Graph™ LC₅₀ calculator (AAT Bioquest Inc., Sunnyvale, CA, USA).

2.4. Analysis of programmed cell death

Both cell lines were cultured in 6-well plates at a concentration of 1.0×10^5 cells/well and starved for 16 h. After starvation, the cells were exposed to bensulide (0, 1, 3, or 5 mg/L) for 48 h and harvested by trypsinization. The harvested cells were resuspended in 100 µL of 1 × annexin binding buffer. Propidium iodide (PI; BD Biosciences, Franklin Lakes, NJ, USA) and annexin V (BD Bioscience) were added (5 µL each) to stain the apoptotic cells. Apoptotic cells were analyzed using a BD Accuri C6 Plus Flow Cytometer (BD Biosciences). Interference to the fluorescence signals between PI and annexin V was compensated. Experiments were conducted in triplicate.

2.5. Extraction of total RNA and analysis of mRNA expression

Both cell lines were seeded into 60-mm culture plates (3.0×10^5 cells/well) and starved for 16 h. Cells treated with 0 or 5 mg/L bensulide



for 24 h were used for total RNA extraction using TransZol Up (TransGen Biotech, Beijing, China). The extracted total RNA was analyzed using SPECTROstar Nano (BMG Labtech, Ortenberg, Germany) to identify purity and concentration. Reverse transcription PCR was conducted to synthesize complementary DNA (cDNA) using random primers (Invitrogen, Massachusetts, USA), AccuPower RT PreMix (Bioneer, Daejeon, Korea), and Oligo dT primers (Bioneer). Synthesized cDNA, SYBR Green (Sigma-Aldrich), ROX reference dye (Invitrogen), and specific primer sets were used for RT-qPCR. Detailed information regarding the specific primer sets is provided in Table 2. mRNA transcription was analyzed using the 2^{-ΔΔ}C_T method (Livak and Schmittgen, 2001). GAPDH, a housekeeping gene, was used to normalize the cycle threshold (C_T) values of all genes. Python with the Seaborn library was used to create a heatmap. Experiments were conducted in triplicate.

2.6. Western blotting

Both cell lines were seeded into 60-mm culture plates (3.0×10^5 cells/well) and starved in serum-free medium. The starved cells were exposed to 0, 1, 3, and 5 mg/L bensulide for 30 min to analyze the phosphorylation of MAPK signaling pathway members. To analyze cell division cycle-related proteins, cells were exposed to 0 and 5 mg/L bensulide for 48 h. After bensulide exposure, lysis buffer was used to collect whole protein extracts. Bradford protein assay (Bio-Rad, Hercules, CA, USA) was used to analyze protein concentrations. Proteins were separated by SDS-PAGE and transferred to nitrocellulose membranes.

Fig. 1. Effects of bensulide on cell survival in pTr and pLE cells. [A] Relative cell viability of pTr and pLE cells was analyzed. LC₅₀ values were determined. [B] Apoptotic cell death was analyzed under bensulide exposure. [C-E] Relative cell populations of [C] normal cells, [D] early apoptotic cells, and [E] late apoptotic cells were analyzed. The graph presents the result of flow cytometry dot plots at left. [F-G] Relative mRNA expression levels of [F] BAX and [G] BAK in pTr and pLE cells after 24 h bensulide exposure were identified. Statistical significance is indicated by asterisks (*p < 0.05; **p < 0.01; ***p < 0.001).

Proteins on the membrane were incubated with antibodies for 16 h. Following incubation with primary antibody, peroxidase-labeled goat anti-rabbit and anti-mouse antibodies were used as secondary antibodies. Fluorescence signals of peroxidase were detected. All proteins were normalized to β -actin or GAPDH, housekeeping proteins. This experiment was performed in triplicate.

2.7. Analysis of mitochondrial function

The MMP of both cell types after bensulide exposure was analyzed using the Mitochondria Staining Kit (Catalog No. CS0390, Sigma-Aldrich). After starvation for 16 h and treatment with bensulide for 48 h, the cells were stained with JC-1 dye and suspended in 1 × JC-1 buffer. A BD Accuri C6 Plus Flow cytometer was used to detect fluorescence signals. Experiments were conducted in triplicate.

2.8. Analysis of free Ca^{2+} levels in mitochondria

Cells were harvested from 6-well plate (1.0×10^5 cells/well) and stained with 3 μM Rhod-2 AM dye (Catalog No. R1244, Invitrogen) diluted with HBSS, without calcium, magnesium, or phenol red media (Catalog No. 14175095, Gibco™, Waltham, MA, USA). A BD Accuri C6 Plus Flow cytometer was used for flow cytometry. Experiments were conducted in triplicate.

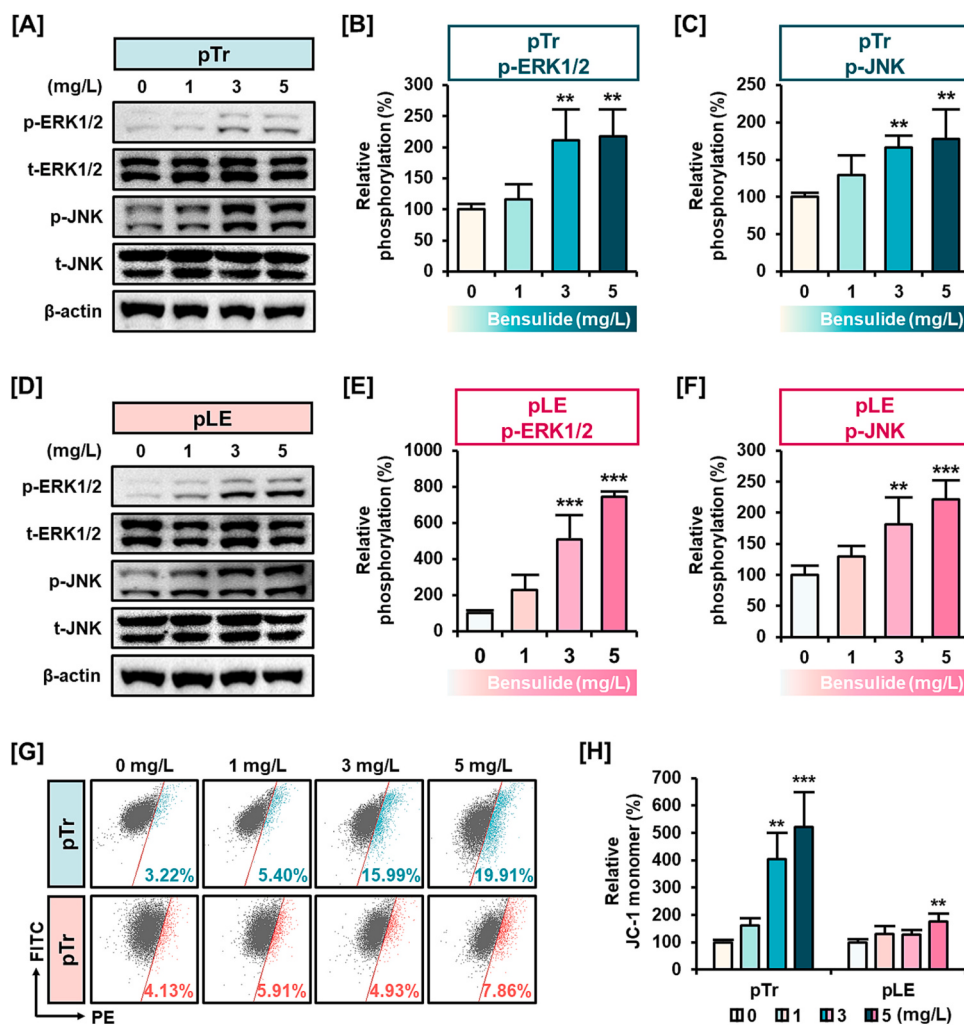


Fig. 2. Effects of bensulide on MAPK signaling and mitochondria in pTr and pLE cells. [A] Phosphorylation of MAPK signaling molecules was identified in pTr cells. [B–C] Relative phosphorylation of [B] ERK1/2 and [C] JNK was identified in pTr cells. [D] Activation of ERK1/2 and JNK was analyzed in pLE cells. [E–F] In pLE cells, phosphorylation levels of [E] ERK1/2 and [F] JNK were examined. Phosphorylation levels were calculated as the ratio of phosphorylated form to the total form of each molecule. [G] Flow cytometry dot plot showing MMP disruption after bensulide exposure. [H] Levels of JC-1 monomer, which reflects the collapse of MMP, increased after bensulide exposure in pTr and pLE cells. The graph presents the result of the flow cytometry dot plot at left. Statistical significance is indicated by asterisks (** $p < 0.01$; *** $p < 0.001$).

2.9. Analysis of cytosolic free Ca^{2+} levels

Cells were prepared in 6-well plates (1.0×10^5 cells/well) and starved in serum-free media for 16 h, then exposed to bensulide (0, 1, 3, and 5 mg/L) for 48 h and harvested. Fluo-4 AM dye (catalog no. F14201; Invitrogen) was diluted in DMSO. Both harvested cell lines were incubated with serum-free media containing Fluo-4 AM dye (3 μM) and rinsed with 1 \times PBS. A BD Accuri C6 Plus Flow cytometer was used to detect fluorescence of the stained cells. Experiments were conducted in triplicate.

2.10. Analysis of cell proliferation rate

A BrdU Cell Proliferation ELISA Kit (Catalog No. 11647229001, Roche) was used to analyze cell proliferation rates. Both cell types were added to 96-well plates (2.7×10^3 cells/well), starved, and then treated with bensulide, as described above. The treated cells were exposed to bromodeoxyuridine (BrdU) for 2 h and 30 min. After incubation, the cells were fixed in a fixation solution for 30 min and incubated with an anti-BrdU antibody for 1 h 30 min. The TMB substrate was added and BrdU-positive cells were measured using an ELISA plate reader at 370 nm–492 nm. Experiments were conducted in triplicate.

2.11. Analysis of cell-division cycle progression

Both cell lines were cultured in 6 well plates (1.0×10^5 cells/well). After serum-free starvation for 16 h and bensulide (0, 1, 3, and 5 mg/L)

treatment for 48 h, the cells were harvested. Elimination of RNA and PI staining was performed. A BD Accuri C6 Plus Flow cytometer was used to analyze PI signals. Experiments were conducted in triplicate. Detailed information concerning the method is described in a previous study (Kim et al., 2023).

2.12. Analysis of cell migration

Both cell types were seeded into a Culture-Insert 2 Well μ -dish at a concentration of 2.8×10^4 cells/well (Catalog No. 81176, ibidi GmbH, Gräfelfing, Germany). A vehicle (0.05% DMSO) or 5 mg/L bensulide solution was used to expose the cells. Images were captured using a Leica DFC550 digital camera (Leica Camera AG, Wetzlar, Germany) every 2 h after the insert was removed. The area of the wound was analyzed using ImageJ software. Experiments were conducted in triplicate.

2.13. Analysis of spheroid formation

Both cell lines were seeded on top of a 100-mm culture dish plate. They hung, suspended, from the top of the dish. The drops were treated with 0 or 5 mg/L bensulide. Spheroid formation was detected using a Leica DFC550 digital camera (Leica Camera AG) after 48 h incubation in a 37°C CO_2 incubator. The spheroid size and number of colonies were analyzed using ImageJ software. Experiments were conducted in triplicate.

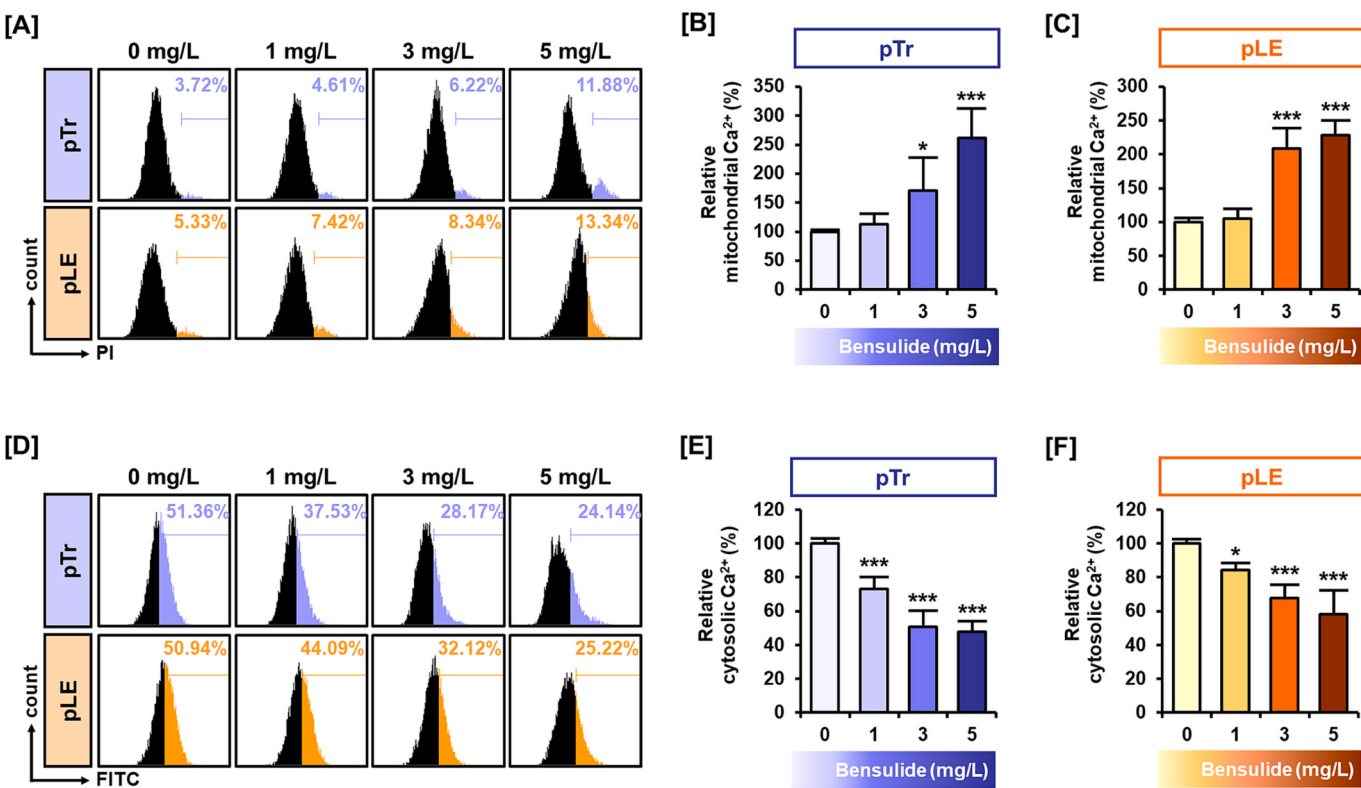


Fig. 3. Effects of bensulide on intracellular Ca²⁺ levels in pTr and pLE cells. [A] Mitochondrial Ca²⁺ levels were identified after bensulide exposure. [B—C] Relative levels of mitochondrial Ca²⁺ were increased in both [B] pTr and [C] pLE cells. [D] Cytosolic Ca²⁺ levels were analyzed under bensulide exposure. [E-F] Decreased cytosolic Ca²⁺ levels were confirmed in [E] pTr and [F] pLE cells. Statistical significance is indicated by asterisks (*p < 0.05; ***p < 0.001).

2.14. Statistical analysis

The SAS program (SAS Institute, Cary, NC, USA) was used to identify statistical significance between control and experimental groups. The SAS program included one-way analysis of variance (ANOVA) with the general linear model (PROG-GLM). An asterisk indicates statistical significance and indicates a p-value <0.05 (*).

3. Results

3.1. Bensulide reduces cell viability via programmed cell death

Cell viability was evaluated at various concentrations of bensulide (0, 0.5, 1, 2, 3, 5, 8, 10, 15, and 20 mg/L). The LC₅₀ values were determined as 5.21 mg/L for pTr and 6.49 mg/L for pLE cells (Fig. 1A). Therefore, the highest concentration used in subsequent experiments was set at 5 mg/L, which was lower than the LC₅₀ value of both cells. Subsequently, the effects of bensulide on apoptosis induction were identified (Fig. 1B). During bensulide exposure, the number of normal cells decreased, and the population of apoptotic cells increased (Fig. 1C-E). Cells with early apoptosis increased to 182.11% (p < 0.05) for pTr and 213.65% (p < 0.001) for pLE cells after exposure to 5 mg/L bensulide (Fig. 1D). After exposure to bensulide, the cell population in the late apoptotic stage increased to 210.28% for pTr and 160.23% for pLE cells (Fig. 1E). In addition, the transcription of *BAX*, a pro-apoptotic factor, was increased to 119.61% (p < 0.01) and 122.05% (p < 0.05) in pTr and pLE cells, respectively, after exposure to 5 mg/L bensulide for 24 h (Fig. 1F). The transcription of *BAK* also increased to 112.17% (p < 0.01) in pLE cells. The transcription of *BAK* did not change significantly in pTr cells. Therefore, bensulide induced the expression of pro-apoptotic factors and programmed cell death. These results implied that bensulide exposure caused programmed cell death and reduced cell viability.

3.2. Bensulide causes MAPK signaling dysregulation and MMP disruption

Various intracellular environmental changes are involved in inducing programmed cell death following exposure to toxic substances. Therefore, the MAPK signaling cascade and mitochondrial membrane potential were investigated after bensulide exposure. In pTr cells, phosphorylated forms of ERK1/2 and JNK were increased to 217.49% (p < 0.01) and 177.92% (p < 0.01), respectively, in response to 5 mg/L bensulide exposure for 30 min (Fig. 2A-C). The phosphorylation of both MAPK proteins in pLE cells increased to 742.87% (p < 0.001) and 221.22% (p < 0.001), respectively, under the same conditions as pTr cells (Fig. 2D-F). MMP disruption was identified by increasing JC-1 monomer levels (Fig. 2G). The relative number of JC-1 monomers increased to 522.45% (p < 0.001) in pTr and 176.77% (p < 0.01) in pLE cells after 5 mg/L bensulide exposure for 48 h (Fig. 2H). These results suggested that bensulide can induce programmed cell death by abnormally activating the MAPK signaling cascade and interfering with mitochondrial function.

3.3. Bensulide dysregulates calcium homeostasis

Mitochondria play important roles not only in generating cellular energy but also in maintaining Ca²⁺ homeostasis in cells. Since it was confirmed that bensulide impairs mitochondrial function in both cell types, we hypothesized that bensulide dysregulates Ca²⁺ homeostasis. Therefore, alterations in Ca²⁺ homeostasis following bensulide exposure were investigated. First, mitochondrial Ca²⁺ levels were identified (Fig. 3A). In pTr and pLE cells, mitochondrial Ca²⁺ levels increased to 261.24% (p < 0.001) and 228.04% (p < 0.001), respectively, after 5 mg/L bensulide exposure (Fig. 3B and C). Next, cytosolic Ca²⁺ levels were evaluated (Fig. 3D). In response to 5 mg/L bensulide exposure, cytosolic Ca²⁺ levels decreased to 47.84% (p < 0.001) in pTr cells (Fig. 3E). Ca²⁺ levels in the cytosol of pLE also dropped to 58.10% (p < 0.001) (Fig. 3F).

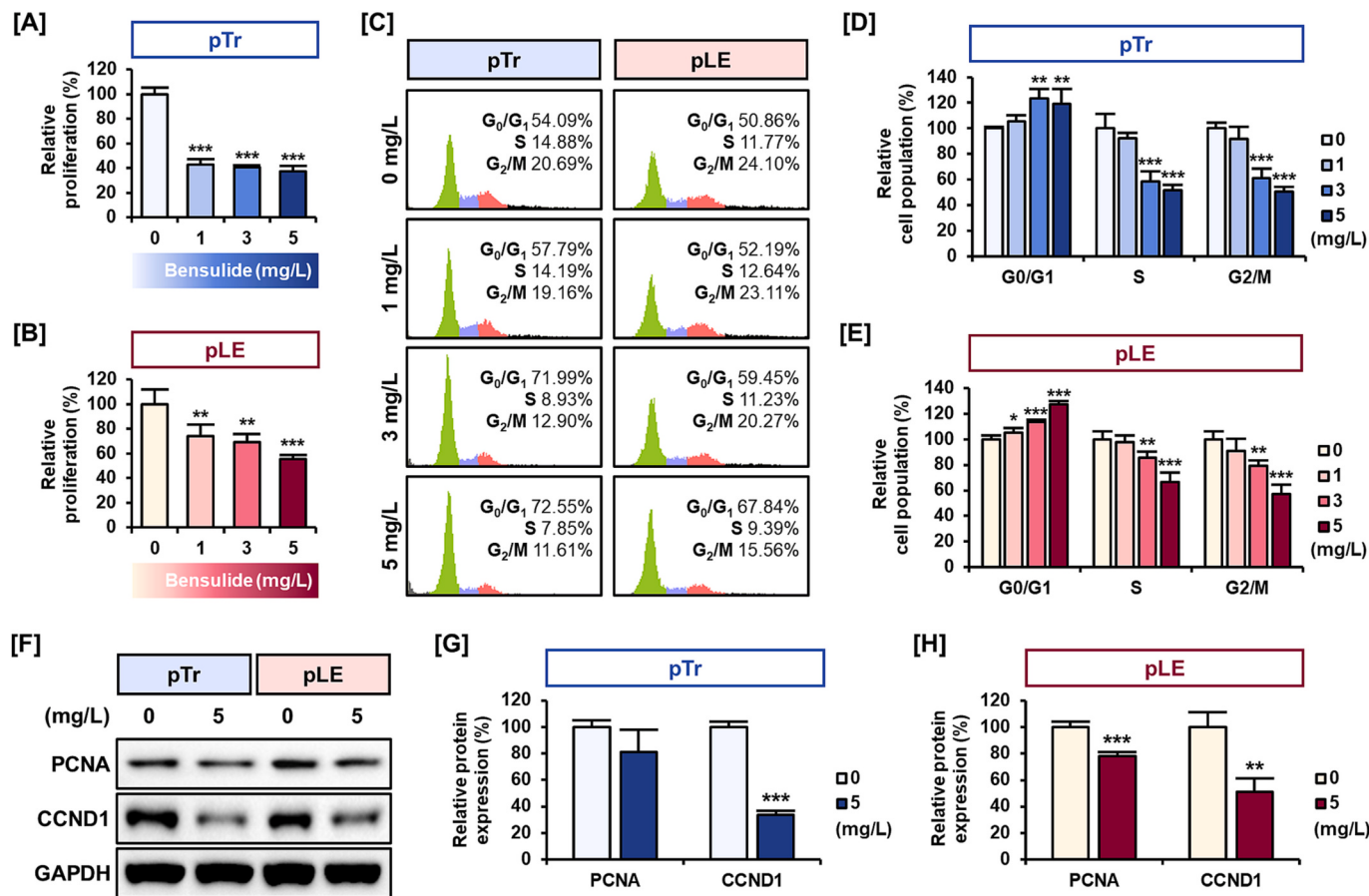


Fig. 4. Effects of bensulide on proliferation and cell cycle progression in pTr and pLE cells. [A-B] The relative proliferation rate of [A] pTr and [B] pLE was visualized through BrdU labeling after bensulide exposure. [C] Cell cycle progression was analyzed by DNA quantification after 48 h of bensulide exposure. [D-E] The populations of G₀/G₁, S, and G₂/M phase cells were analyzed in [D] pTr and [E] pLE cells. The graph shows the flow cytometry histogram on left. [F] Protein expression of PCNA and CCND1 was identified. [G-H] The expression levels of PCNA and CCND1 were analyzed in [G] pTr and [H] pLE cells. The expression levels of each protein were normalized to that of GAPDH. Statistical significance is indicated by asterisks (* $p < 0.05$; ** $p < 0.01$; *** $p < 0.001$).

These results demonstrated that bensulide exposure adversely affects Ca²⁺ homeostasis.

3.4. Bensulide inhibits cell division cycle progression

The antiproliferative effects of bensulide were investigated using BrdU labeling. In both cell lines, it was observed that a concentration of bensulide > 1 mg/L inhibited proliferation. The proliferation rate of pTr and pLE cells decreased to 37.13% ($p < 0.001$) and 55.66% ($p < 0.001$), respectively, after 5 mg/L bensulide exposure (Fig. 4A and B). To investigate which phase of the cell division cycle is related to the anti-proliferative effects of bensulide, PI staining was conducted (Fig. 4C). Cells exposed to 0, 1, 3, and 5 mg/L bensulide were analyzed according to the amount of DNA present. In pTr cells, 5 mg/L bensulide increased the number of cells in G₀/G₁ phase to 119.24% ($p < 0.01$) and decreased the number of cells in S phase to 51.67% ($p < 0.001$) and G₂/M phase to 50.50% ($p < 0.001$) (Fig. 4D). In addition, treatment with 5 mg/L bensulide increased the G₀/G₁ population to 127.39% ($p < 0.001$) and decreased the S and G₂/M populations to 66.44% ($p < 0.001$) and 57.24% ($p < 0.001$), respectively, in pLE cells (Fig. 4E).

Cell division cycle progression is regulated by several proteins. Therefore, we identified the expression levels of PCNA and CCND1, which are cell-division cycle-related proteins, after bensulide exposure (Fig. 4F). CCND1 protein expression decreased to 33.87% ($p < 0.001$), but PCNA expression was not significantly different in pTr cells after exposure to 5 mg/L bensulide for 48 h (Fig. 4G). However, protein expression of PCNA and CCND1 in pLE cells decreased to 78.22% ($p <$

0.001) and 50.92% ($p < 0.01$), respectively, in response to 5 mg/L bensulide. Collectively, bensulide decreased the level of cell division cycle-related proteins and arrested cell division cycle progression and proliferation.

3.5. Effects of bensulide on cell migration and aggregation ability

Various cytotoxic effects of bensulide were also evaluated. These results suggested that bensulide may impair the functioning of both cell types as a result of its cytotoxic effects. First, migration assays were conducted to evaluate the migratory ability of both cell lines (Fig. 5A). Migration progressed in both the control and 5 mg/L bensulide-treated groups. However, after 8 h of wound formation in pTr cells, the wound area in the control group decreased to 11.95%, but the treated group exhibited a decrease of only 32.69% ($p < 0.001$) (Fig. 5B). The wound area of the pLE cells decreased to 31.60% and 38.03% ($p < 0.05$) in the control and treated groups, respectively (Fig. 5C). This result suggested that the migration ability of pLE cells also decreased after bensulide exposure.

Second, spheroid formation was investigated by quantifying three factors: spheroid size, colony number in spheroids, and average size of individual colonies (Fig. 5D). Spheroid formation was analyzed to identify the adverse effects of bensulide on both cell types in an *in vivo*-like state. The size of spheroids and number of colonies of pTr cells treated with 5 mg/L bensulide increased to 134.83% ($p < 0.01$) and 188.13% ($p < 0.001$), respectively, whereas the size of individual colonies decreased to 65.51% ($p < 0.01$) (Fig. 5E). pLE cells exposed to 5

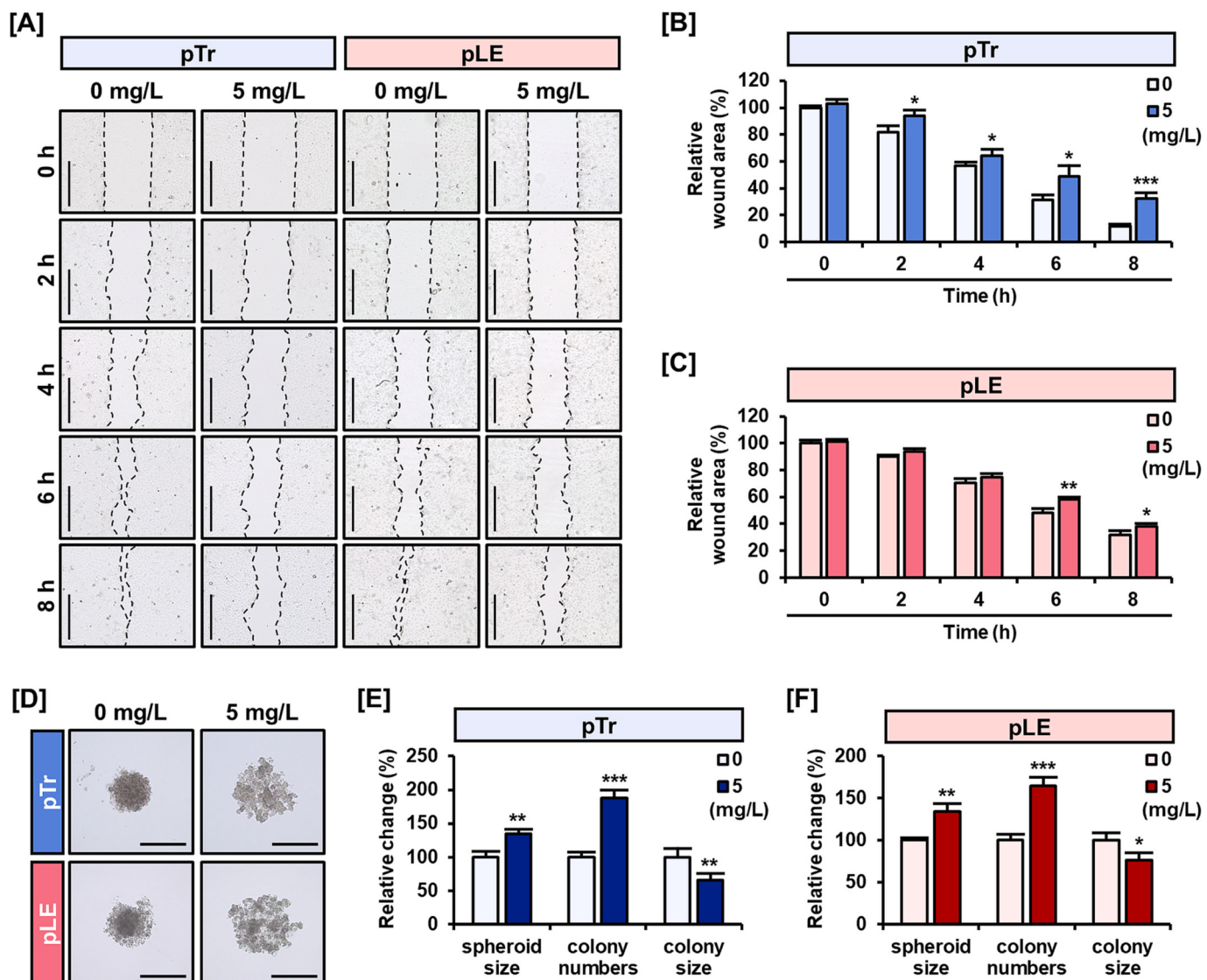


Fig. 5. Effects of bensulide on migration and aggregation ability in pTr and pLE cells. [A] Images of wound healing were acquired over time in pTr and pLE cells. The scale bar represents 500 μ m. [B–C] Wound areas in [B] pTr and [C] pLE cells were analyzed. For each time-point, the wound size of the 0 mg/L treated group and 5 mg/L treated group were compared. [D] Aggregation ability was evaluated by spheroid formation. [E–F] The size of whole spheroids, number of colonies, and the size of each colony were analyzed in [E] pTr and [F] pLE. Statistical significance is indicated by asterisks (* $p < 0.05$; ** $p < 0.01$; *** $p < 0.001$).

mg/L bensulide formed 134.27% ($p < 0.01$) larger spheroids compared to the control group, and the number of colonies constituting the spheroid increased to 164.82% ($p < 0.001$). The average size of each colony decreased by 76.22% ($p < 0.05$) after bensulide exposure (Fig. 5F). Both cell types formed loose spheroids after bensulide exposure.

3.6. Effects of bensulide on pregnancy-related factors

Both cell types are closely related to implantation in the early pregnancy stage in pigs. In addition, the transcription of receptor genes related to each factor should be regulated appropriately. Therefore, we identified gene expression related to pregnancy-related factors after bensulide exposure of 5 mg/L for 24 h. In pTr, the mRNA expression of *ESR2*, *CASP1*, and *RXFP1* decreased (Fig. 6A). The mRNA expression of *ESR2* and *CASP1* in pLE cells decreased in pTr cells after bensulide exposure. In addition, *ESR1* and *PTGIR* were downregulated in pLE cells (Fig. 6B). Transcription of *ESR1* and *PTGIR* in pTr and expression of *RXFP1* in pLE were not significantly different after bensulide exposure. These gene expression profiles suggested that bensulide dysregulates the

expression of pregnancy-related factors and can induce implantation failure in early stages of pregnancy.

4. Discussion

This study aimed to identify the intracellular mechanisms underlying the toxic effects of bensulide on implantation-related cells. As bensulide has characteristics such as a long half-life and potential for adsorption by organisms, it may cause unexpected adverse effects on non-target organisms. Therefore, various *in vivo* and *in vitro* studies have been conducted, and toxic effects on reproduction and development have been identified. To identify the intracellular mechanisms of bensulide's toxic effects, both cell types were exposed to bensulide for up to 48 h. Various environments and functions in cells were evaluated after exposure to bensulide, and the results of the present study clarified the mechanism of toxicity involving implantation-related cells. The adverse effects of bensulide on both cell types are schematically presented in Fig. 7.

The LC₅₀ values of bensulide on pTr and pLE were determined by the MTT assay. All experiments conducted in this study were performed using <5 mg/L bensulide, which was lower than the LC₅₀ value

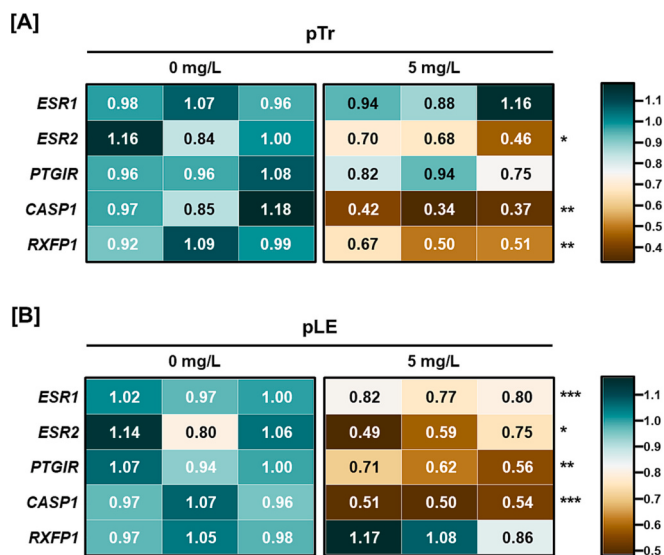


Fig. 6. Heatmap of function-related gene expression profiles in pTr and pLE cells under bensulide exposure. [A- B] The mRNA expression of *ESR1*, *ESR2*, *PTGIR*, *CASP1*, and *RXFP1* was evaluated in [A] pTr and [B] pLE cells. The color of the heatmap shows the -fold change in gene expression level compared to the average value of each gene in the 0 mg/L bensulide-treated group. Statistical significance is indicated by asterisks (* $p < 0.05$; ** $p < 0.01$; *** $p < 0.001$).

determined for both cell lines using the MTT assay. We observed the induction of apoptosis and programmed cell death in both cell lines. The mRNA transcription of pro-apoptotic factors (*BAX* and *BAK*) was also identified. ERK1/2 and JNK phosphorylation was also investigated because *BAX* and *BAK* are related to the hyperactivation of ERK1/2 and JNK signals (Sugiura et al., 2021; Papadakis et al., 2006). We noted that ERK1/2 and JNK phosphorylation and *BAX* and *BAK* activation-induced apoptosis are associated with mitochondrial function (Tsuruta et al., 2004; Cook et al., 2017). Since mitochondrial function is closely related to MMP, changes in MMP following exposure to bensulide were identified. In addition, mitochondrial function is related to cellular Ca^{2+} homeostasis (Romero-Garcia and Prado-Garcia, 2019). Ca^{2+} overloaded mitochondria, and the concentration of Ca^{2+} in the cytoplasm decreased after bensulide exposure. Therefore, these results suggest that exposure to bensulide causes problems with the ability to regulate Ca^{2+} homeostasis in mitochondria and induce apoptotic signals, thereby reducing cell viability.

The growth inhibitory effect of bensulide was reported in an *in vitro* study. Therefore, we hypothesized that the proliferation rate and cell division cycle were also affected by bensulide treatment in both cell lines. The results of cell division cycle analysis revealed a reduction in S and G₂/M phase populations. Following cell division cycle analysis, PCNA and CCND1 proteins related to cell division cycle progression were identified. The levels of CCND1 and PCNA were reduced after bensulide exposure. CCND1 is an important factor in cell division cycle progression. During the cell division cycle, the G₁ to S phase transition does not occur when CCND1 level are decreased (Guardavaccaro et al., 2000). In addition, PCNA is essential for the DNA replication process, the main event in the S phase of the cell division cycle (Strzalka and Ziemiowicz, 2011). Therefore, decreased expression of PCNA in response to bensulide treatment prevents cell division cycle progression. These results supported our hypothesis that bensulide also exhibits growth inhibitory effects in both cell types and suggested that the cell division cycle can be stopped by inhibiting the transition from G₁ to S.

Finally, we investigated how the function of pTr and pLE cells exposed to bensulide was affected. Migration assays and spheroid formation were conducted to evaluate the migration and aggregation abilities, respectively. The results of these studies showed that bensulide

compromised the migration and aggregation abilities of pTr and pLE cells. The migration and aggregation abilities are closely related to successful implantation between the trophectoderm and uterine luminal endometrium (Grewal et al., 2008). The migration and aggregation ability of cells was closely related to the regulation of intracellular Ca^{2+} levels (Yang and Huang, 2005; Ko et al., 2001). Therefore, we propose that impaired migration and aggregation are associated with abnormal Ca^{2+} levels caused by exposure to bensulide. In addition, pTr and pLE cells tightly regulate the expression of various factors and their receptors for successful implantation. Therefore, mRNA expression related to implantation signaling was evaluated in pTr and pLE cells after bensulide exposure for 24 h. The mRNA expression of estrogen receptor (*ESR1* and *ESR2*), prostaglandin receptor (*PTGIR*), caspase 1 (*CASP1*), and relaxin family peptide receptor 1 (*RXFP1*) was downregulated upon bensulide exposure. Estrogen and prostaglandin signals are essential for implantation (Robertshaw et al., 2016; Buchanan et al., 1999; Vilella et al., 2013). However, the absence of estrogen signaling is related to infertility in females (Lubahn et al., 1993). Furthermore, the lack of prostaglandin signals affects the survival of porcine conceptuses and causes termination of pregnancy before implantation (Kraeling et al., 1985; Kaczynski et al., 2018). During implantation, various cytokines are secreted between the conceptus and uterine luminal endometrium, and *CASP1* is expressed to activate related cytokines (Ross et al., 2003). Contrary to previous studies showing that *CASP1* expression increases during implantation (Ashworth et al., 2010), *CASP1* expression in pTr and pLE cells under bensulide exposure decreased. These results suggested that bensulide impairs implantation-related functions.

This study demonstrated the adverse effects of bensulide on implantation-related cells. To our knowledge, this is the first study to document the mechanisms of intracellular toxic effects and alterations in terms of implantation-related gene expression. These results suggested that bensulide induces apoptosis and cell division cycle arrest via disruption of Ca^{2+} homeostasis, causing mitochondrial dysfunction and dysregulation of mRNA and protein expression. These alterations in intracellular responses cause loss of functions, such as migration, aggregation, and dysregulation of pregnancy-related factors in pTr and pLE cells. Based on these results, we propose that bensulide may induce implantation failure by disrupting the cell function and interfering with cell-cell interactions between the trophectoderm and the uterine luminal endometrium during implantation. pTr and pLE are porcine-derived cells, and pigs have implantation-related functions similar to those of humans (Baryla et al., 2019; Waclawik, 2011). Therefore, we suggest that the effects of bensulide identified in the present study can be applied to humans. However, this study had certain limitations: (1) The present study did not provide information about *in vivo* studies. Therefore, it did not establish a direct interaction between trophectoderm and uterine luminal cells, as in the actual pregnancy process. Hence, we suggest that *vivo* studies be conducted using animal models. (2) This study identified cellular responses to bensulide at the molecular level. However, our results do not fully demonstrate the relationship between these responses. (3) Alteration of pregnancy-related factors, with regard to protein levels, has not been fully verified. Therefore, further research is required to verify the relationship between intracellular reactions, either by processing inhibitors or by controlling the expression of related genes. In addition, identifying alterations in the protein level of each pregnancy-related factor after bensulide exposure is also worth exploring.

5. Conclusions

Overall, the present study demonstrated the adverse effects of bensulide and its mechanisms of action in implantation-related cells. Indeed, bensulide caused activation of MAPK signaling pathways and also Ca^{2+} overload in mitochondria. In addition, bensulide dysregulated Ca^{2+} homeostasis disrupting MMP and caused cell division cycle arrest and programmed cell death by dysregulating the transcription of mRNA

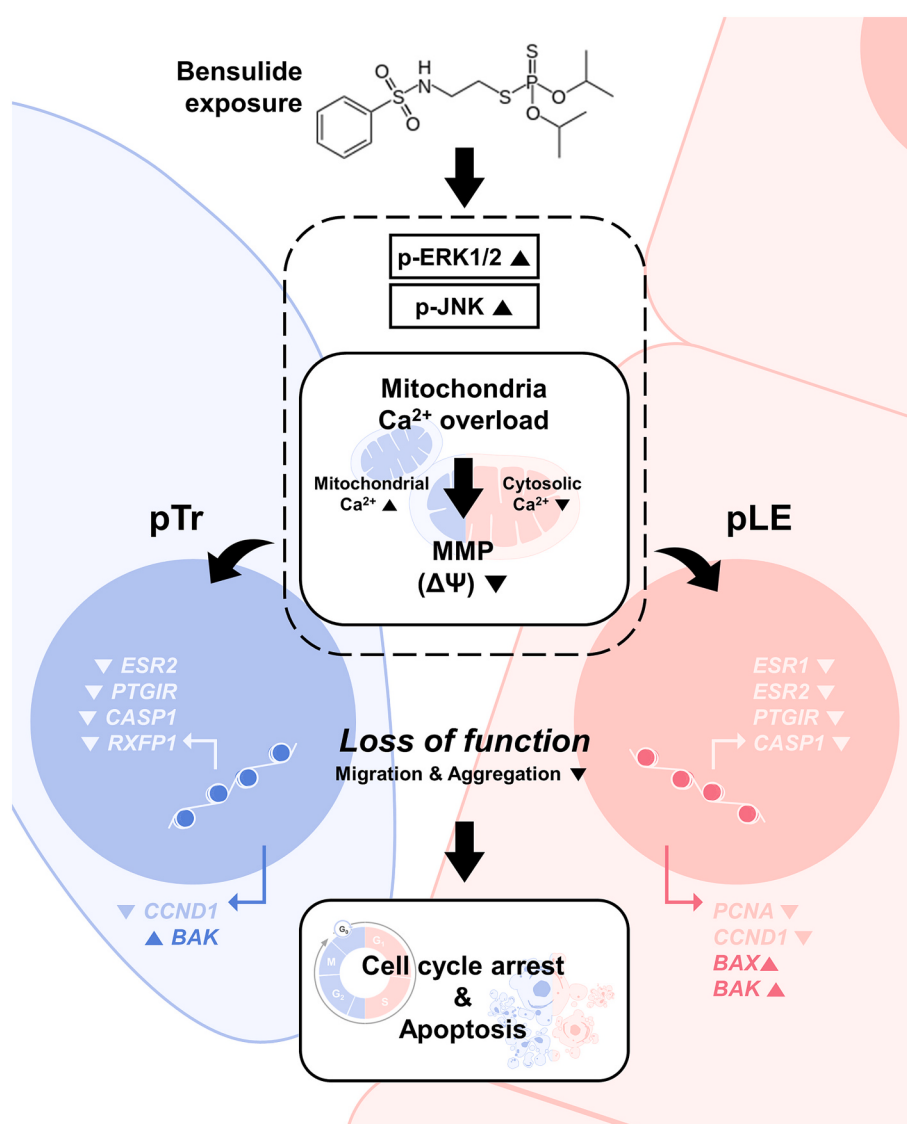


Fig. 7. Illustrations of the effects of bensulide on the intracellular system of pTr and pLE cells. Bensulide induces activation of MAPK signaling molecules ERK1/2 and JNK. Ca²⁺ was overloaded in mitochondria. Intracellular Ca²⁺ homeostasis and MMP were disrupted. The function-related genes of pTr and pLE (*ESR1*, *ESR2*, *PTGIR*, *CASP1*, and *RXFP1*) were dysregulated under bensulide exposure. Finally, bensulide caused loss of function including migration and aggregation ability, and induced cell cycle arrest and apoptosis.

and proteins of related factors. To our knowledge, this is the first report regarding the intracellular mechanisms of the adverse effects of bensulide on implantation-related cells. Even though the concentrations of bensulide used in this study could not fully reflect the environmental situation, however, they were set for mechanistic study of the hazardous effect of bensulide. Also, this study identified the intracellular mechanism of bensulide, and there is a limit to identifying the exact toxic effect of bensulide *in vivo*. Therefore, in the future, it is necessary to verify the action of bensulide in non-targeted organisms *in vivo* at environmentally relevant concentrations.

Declaration of Competing Interest

The authors declare that there are no conflicts of interest.

Acknowledgements

This research was supported by the National Research Foundation of Korea (NRF) grant funded by the Korea government (MSIT) (grant number: 2021R1A2C2005841 & 2021R1C1C1009807). This research was also supported by the Health Fellowship Foundation. Also, this research was supported by Basic Science Research Program through the National Research Foundation of Korea (NRF) funded by the Ministry of

Education (grant number: 2019R1A6A1A10073079).

References

- Antonious, G.F., 2010. Mobility and half-life of bensulide in agricultural soil. *J. Environ. Sci. Health B* 45, 1–10.
- Ashworth, M.D., Ross, J.W., Stein, D.R., White, F.J., Desilva, U.W., Geisert, R.D., 2010. Endometrial caspase 1 and interleukin-18 expression during the estrous cycle and peri-implantation period of porcine pregnancy and response to early exogenous estrogen administration. *Reprod. Biol. Endocrinol.* 8, 33.
- Baryla, M., Kaczynski, P., Goryszewska, E., Riley, S.C., Waclawik, A., 2019. Prostaglandin F(2alpha) stimulates adhesion, migration, invasion and proliferation of the human trophoblast cell line HTR-8/SVneo. *Placenta* 77, 19–29.
- Bensulide, I., 2006. O. Pesticides, Reregistration Eligibility Decision for Bensulide.
- Buchanan, D.L., Setiawan, T., Lubahn, D.B., Taylor, J.A., Kurita, T., Cunha, G.R., Cooke, P.S., 1999. Tissue compartment-specific estrogen receptor-alpha participation in the mouse uterine epithelial secretory response. *Endocrinology* 140, 484–491.
- Cook, S.J., Stuart, K., Gilley, R., Sale, M.J., 2017. Control of cell death and mitochondrial fission by ERK1/2 MAP kinase signalling. *FEBS J.* 284, 4177–4195.
- Donley, N., 2019. The USA lags behind other agricultural nations in banning harmful pesticides. *Environ. Health* 18, 44.
- Eskenazi, B., Harley, K., Bradman, A., Weltzien, E., Jewell, N.P., Barr, D.B., Furlong, C.E., Holland, N.T., 2004. Association of in utero organophosphate pesticide exposure and fetal growth and length of gestation in an agricultural population. *Environ. Health Perspect.* 112, 1116–1124.
- Grewal, S., Carver, J.G., Ridley, A.J., Mardon, H.J., 2008. Implantation of the human embryo requires Rac1-dependent endometrial stromal cell migration. *Proc. Natl. Acad. Sci. U. S. A.* 105, 16189–16194.

- Guardavaccaro, D., Corrente, G., Covone, F., Micheli, L., D'Agnano, I., Starace, G., Caruso, M., Tirone, F., 2000. Arrest of G1/S progression by the p53-inducible gene PC3 is Rb dependent and relies on the inhibition of cyclin D1 transcription. *Mol. Cell. Biol.* 20, 1797–1815.
- Haith, D.A., Rossi, F.S., 2003. Risk assessment of pesticide runoff from turf. *J. Environ. Qual.* 32, 447–455.
- Hu, P., Vinturache, A., Li, H., Tian, Y., Yuan, L., Cai, C., Lu, M., Zhao, J., Zhang, Q., Gao, Y., Liu, Z., Ding, G., 2020. Urinary organophosphate metabolite concentrations and pregnancy outcomes among women conceiving through in vitro fertilization in Shanghai, China. *Environ Health Perspect* 128, 97007.
- Ka, H., Jaeger, L.A., Johnson, G.A., Spencer, T.E., Bazer, F.W., 2001. Keratinocyte growth factor is up-regulated by estrogen in the porcine uterine endometrium and functions in trophectoderm cell proliferation and differentiation. *Endocrinology* 142, 2303–2310.
- Kaczynski, P., Baryla, M., Goryszewska, E., Bauersachs, S., Waclawik, A., 2018. Prostaglandin F2alpha promotes embryo implantation and development in the pig. *Reproduction* 156, 405–419.
- Kim, M., An, G., Lim, W., Song, G., 2022. Fluroxypyrr-1-methylheptyl ester induced ROS production and mitochondrial apoptosis through the MAPK signaling cascade in porcine trophectoderm and uterine luminal epithelial cells. *Pestic. Biochem. Physiol.* 187, 105196.
- Kim, M., Park, J., An, G., Lim, W., Song, G., 2023. Pendimethalin exposure disrupts mitochondrial function and impairs processes related to implantation. *Reproduction* 165, 491–505.
- Kleinstreuer, N.C., Judson, R.S., Reif, D.M., Sipes, N.S., Singh, A.V., Chandler, K.J., Dewoskin, R., Dix, D.J., Kavlock, R.J., Knudsen, T.B., 2011. Environmental impact on vascular development predicted by high-throughput screening. *Environ. Health Perspect.* 119, 1596–1603.
- Ko, K.S., Arora, P.D., Bhide, V., Chen, A., McCulloch, C.A., 2001. Cell-cell adhesion in human fibroblasts requires calcium signaling. *J. Cell Sci.* 114, 1155–1167.
- Kraeling, R.R., Rampacek, G.B., Fiorello, N.A., 1985. Inhibition of pregnancy with indomethacin in mature gilts and prepuberal gilts induced to ovulate. *Biol. Reprod.* 32, 105–110.
- Livak, K.J., Schmittgen, T.D., 2001. Analysis of relative gene expression data using real-time quantitative PCR and the 2(-Delta Delta C(T)) method. *Methods* 25, 402–408.
- Lopez-Garcia, M., Romero-Gonzalez, R., Garrido-Frenich, A., 2019. Monitoring of organophosphate and pyrethroid metabolites in human urine samples by an automated method (TurboFlow) coupled to ultra-high performance liquid chromatography-Orbitrap mass spectrometry. *J. Pharm. Biomed. Anal.* 173, 31–39.
- Lubahn, D.B., Moyer, J.S., Golding, T.S., Couse, J.F., Korach, K.S., Smithies, O., 1993. Alteration of reproductive function but not prenatal sexual development after insertional disruption of the mouse estrogen receptor gene. *Proc. Natl. Acad. Sci. U. S. A.* 90, 11162–11166.
- Mallick, B., Rana, S., Ghosh, T.S., 2023. Role of herbicides in the decline of butterfly population and diversity. *J. Exp. Zool. A Ecol. Integr. Physiol.* 339, 346–356.
- McCorkle, F.M., Chambers, J.E., Yarbrough, J.D., 1977. Acute toxicities of selected herbicides to fingerling channel catfish, *Ictalurus punctatus*. *Bull. Environ. Contam. Toxicol.* 18, 267–270.
- Nakhjavani, B., Bland, J., Khosravifard, M., 2021. Optimization of a multiresidue analysis of 65 pesticides in surface water using solid-phase extraction by LC-MS/MS. *Molecules* 26.
- Papadakis, E.S., Finegan, K.G., Wang, X., Robinson, A.C., Guo, C., Kayahara, M., Tournier, C., 2006. The regulation of Bax by c-Jun N-terminal protein kinase (JNK) is a prerequisite to the mitochondrial-induced apoptotic pathway. *FEBS Lett.* 580, 1320–1326.
- Park, W., Park, S., Lim, W., Song, G., 2021. Bifenthrin reduces pregnancy potential via induction of oxidative stress in porcine trophectoderm and uterine luminal epithelial cells. *Sci. Total Environ.* 784, 147143.
- Park, J., An, G., Lim, W., Song, G., 2022. Dinitramine induces implantation failure by cell cycle arrest and mitochondrial dysfunction in porcine trophectoderm and luminal epithelial cells. *J. Hazard. Mater.* 435, 128927.
- Robertshaw, I., Bian, F., Das, S.K., 2016. Mechanisms of uterine estrogen signaling during early pregnancy in mice: an update. *J. Mol. Endocrinol.* 56, R127–R138.
- Romero-Garcia, S., Prado-Garcia, H., 2019. Mitochondrial calcium: transport and modulation of cellular processes in homeostasis and cancer (review). *Int. J. Oncol.* 54, 1155–1167.
- Ross, J.W., Malayer, J.R., Ritchey, J.W., Geisert, R.D., 2003. Characterization of the interleukin-1beta system during porcine trophoblastic elongation and early placental attachment. *Biol. Reprod.* 69, 1251–1259.
- Safety, A., European Food, Ardizzone, M., Binaglia, M., Cottrill, B., Cugier, J.P., Ferreira, L., Ruiz, J.A., Gomez, Innocenti, M., Ioannidou, S., Puente, S., Lopez, Merten, C., Nikolic, M., Savoini, G., 2019. Animal dietary exposure: overview of current approaches used at EFSA. *EFSA J.* 17, e05896.
- Shellenberger, T.E., Newell, G.W., Bridgman, R.M., Barbaccia, J., 1965. A subacute toxicity study of N-(2-mercaptoethyl) benzenesulfonamide S-(O,O-diisopropyl phosphorodithioate) and phthalimidomethyl-O,O-dimethyl phosphorodithioate with Japanese quail. *Toxicol. Appl. Pharmacol.* 7, 550–558.
- Strzalka, W., Ziemiennowicz, A., 2011. Proliferating cell nuclear antigen (PCNA): a key factor in DNA replication and cell cycle regulation. *Ann. Bot.* 107, 1127–1140.
- Sugiura, R., Satoh, R., Takasaki, T., 2021. ERK: a double-edged sword in Cancer. ERK-dependent apoptosis as a potential therapeutic strategy for Cancer. *Cells* 10.
- Tsuruta, F., Sunayama, J., Mori, Y., Hattori, S., Shimizu, S., Tsujimoto, Y., Yoshioka, K., Masuyama, N., Gotoh, Y., 2004. JNK promotes Bax translocation to mitochondria through phosphorylation of 14-3-3 proteins. *EMBO J.* 23, 1889–1899.
- Vilella, F., Ramirez, L., Berlanga, O., Martinez, S., Alama, P., Meseguer, M., Pellicer, A., Simon, C., 2013. PGE2 and PGF2alpha concentrations in human endometrial fluid as biomarkers for embryonic implantation. *J. Clin. Endocrinol. Metab.* 98, 4123–4132.
- Waclawik, A., 2011. Novel insights into the mechanisms of pregnancy establishment: regulation of prostaglandin synthesis and signaling in the pig. *Reproduction* 142, 389–399.
- Wang, G., Johnson, G.A., Spencer, T.E., Bazer, F.W., 2000. Isolation, immortalization, and initial characterization of uterine cell lines: an in vitro model system for the porcine uterus. *In Vitro Cell Dev Biol Anim* 36, 650–656.
- Yang, S., Huang, X.Y., 2005. Ca²⁺ influx through L-type Ca²⁺ channels controls the trailing tail contraction in growth factor-induced fibroblast cell migration. *J. Biol. Chem.* 280, 27130–27137.
- Zilkah, S., Osband, M.E., McCaffrey, R., 1981. Effect of inhibitors of plant cell division on mammalian tumor cells in vitro. *Cancer Res.* 41, 1879–1883.